

Featuring work from the experimental soft condensed matter group of David A. Weitz.

Title: The microfluidic post-array device: high throughput production of single emulsion drops

The microfluidic post-array device, consisting of an array of regularly arranged posts, enables high throughput production of nearly monodisperse emulsion drops from fluids with viscosities ranging from that of water to 1000 times that of water.

As featured in:



See David A. Weitz et al., *Lab Chip*, 2014, 14, 705.

The microfluidic post-array device: high throughput production of single emulsion drops†

Cite this: *Lab Chip*, 2014, 14, 705

E. Amstad,^a S. S. Datta^b and D. A. Weitz^{*ab}

We present a microfluidic device that enables high throughput production of relatively monodisperse emulsion drops while controlling the average size. The device consists of a two-dimensional array of regularly-spaced posts. Large drops of a highly polydisperse crude emulsion are input into the device and are successively split by the posts, ultimately yielding a finer emulsion consisting of smaller, and much more monodisperse drops. The size distribution of the resultant emulsion depends only weakly on the viscosities of the input fluids and allows fluids of very high viscosities to be used. The average size and polydispersity of the drops depend strongly on the device geometry enabling both control and optimization. We use this device to produce drops of a highly viscous monomer solution and subsequently solidify them into polymeric microparticles. The production rate of these devices is similar to that achieved by membrane emulsification techniques, yet the control over the drop size is superior; thus these post-array microfluidic devices are potentially useful for industrial applications.

Received 27th October 2013,
 Accepted 2nd December 2013

DOI: 10.1039/c3lc51213d

www.rsc.org/loc

Introduction

Emulsion drops are used in a variety of applications; for example, they are contained in many food products such as milk,¹ used as vessels to conduct chemical reactions in very small volumes,² and applied as templates to produce microparticles of controlled size and composition.³ One method to produce these drops is through the use of microfluidics; this affords excellent control over the flow of fluids and enables formation of highly monodisperse drops.⁴ However, because the emulsion is formed drop by drop, scale-up to laboratory or even industrial scales is limited.⁵ However, many industrial applications do not require the exceptionally high monodispersity of the drop size achieved with microfluidics; instead, they can tolerate a significant degree of polydispersity. It would therefore be highly beneficial to develop new microfluidic processes that significantly increase the throughput of drop formation even if the high degree of monodispersity of the drops is relaxed. Such a technique would significantly increase the potential for

microfluidics for production of emulsions at laboratory or even industrial scales.

Here, we present a new design of a microfluidic chip which enables high throughput production of emulsions with good control over the average size albeit not the same degree of monodispersity achieved by many microfluidic drop makers. This is accomplished through the use of an array of posts which interrupt the flow of the internal phase leading to the formation of drops at a throughput similar to that achieved by membrane emulsification techniques,^{6,7} yet, with better control over the average size. Moreover, in contrast to standard microfluidic devices this post-array device enables emulsification of fluids with viscosities up to three orders of magnitude larger than that of water. We demonstrate the utility of this device by using it to form drops of a highly viscous monomer solution which are used as templates for the production of polymeric microparticles.

Results and discussion

The microfluidic post-array device is a two dimensional microfluidic chip fabricated from poly(dimethylsiloxane) (PDMS) using standard soft lithography techniques. It consists of arrays of regularly spaced posts; each row contains 50 posts with adjacent rows of posts offset from each other, as shown in Fig. 1. The device has a single inlet and outlet, making its operation simple and convenient.⁸ We inject a crude emulsion, formed through mechanical agitation, into the inlet using a volume-controlled peristaltic pump. The polydisperse drops are forced through the array of posts,

^a School of Engineering and Applied Sciences, Harvard University, Cambridge, Massachusetts, USA. E-mail: weitz@seas.harvard.edu

^b Department of Physics, Harvard University, Cambridge, Massachusetts, USA

† Electronic supplementary information (ESI) available: High-speed camera movies of emulsions with $\eta_d/\eta_c = 6.3$ (S1 and S2) and $\eta_d/\eta_c = 50$ (S3 and S4) that are pushed through a post-array device with square (S1, S3) and rectangular posts (S2, S4). High-speed camera movies of the inlet (S5) and outlet (S6) of a post-array device containing 300 columns of posts. Experimental details are included. See DOI: 10.1039/c3lc51213d

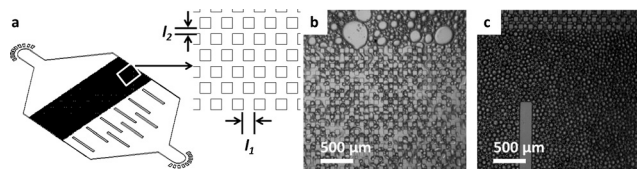


Fig. 1 (a) A schematic illustration of the post-array device; it consists of multiple rows of posts with an inter-post distance l_1 and an inter-row distance l_2 . (b, c) Optical micrographs of the (b) inlet and (c) outlet of a device with $l_1 = 40 \mu\text{m}$ and $l_2 = 20 \mu\text{m}$. Flow direction is from top to bottom.

breaking into many smaller drops in the process. We collect the resulting drops and analyze their size distribution using optical microscopy.

To investigate the influence of shear stress on the size of the resultant drops, we vary the flow rate and viscosity of the crude emulsion. We quantify the performance of the post-array device by measuring the dependence of the average drop size on the capillary number, $Ca = \eta q / (h w \gamma)$, where η is the viscosity of the more viscous fluid, h is the height of the posts, w is the distance between adjacent posts, and γ is the interfacial tension between the two fluids. For a given Ca , drops whose size exceeds a characteristic value become trapped at the posts, and subsequently break into smaller drops; by contrast, drops whose sizes is below this characteristic value bypass the posts without any alteration in their size. This characteristic size decreases with increasing Ca for $Ca < 0.03$; however, it plateaus for $Ca > 0.03$, as shown in Fig. 2a. This crossover value of $Ca = 0.03$ is in excellent agreement with the value obtained in experiments performed with large drops forced to move around a single post in a microfluidic channel;⁹ it also agrees with the results of experiments studying drop formation in T-junctions.^{10,11} To further investigate this behavior, we probe the dependence of the characteristic drop size, for $Ca > 0.03$, on the geometry of the device. We independently vary the inter-post separation within each row l_1 , the inter-row separation l_2 ,

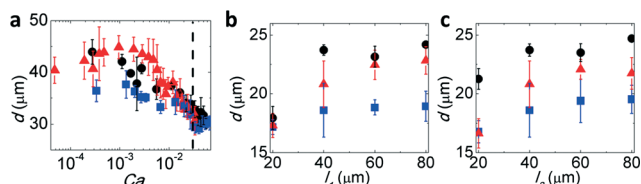


Fig. 2 (a) The influence of the capillary number Ca on the drop size is shown for different types of emulsions; the ratios of the viscosities of the dispersed to the continuous phase η_d/η_c are 6.3 (●), 1.0 (▲), and 0.1 (■). The microfluidic post-array devices consist of 80 columns and 50 rows of square posts. (b, c) The influence of (b) the inter-post distance l_1 , and (c) the inter-row distance l_2 on the characteristic drop size at $Ca > 0.03$. The height of the posts is $20 \mu\text{m}$ (■), $40 \mu\text{m}$ (▲), and $80 \mu\text{m}$ (●). In (b), l_2 is $40 \mu\text{m}$, and in (c) l_1 is $40 \mu\text{m}$. Fluid is injected at 5 ml h^{-1} . The error bars indicate the variance in the size of drops formed in different devices with the same geometry.

and the device height h , as shown in Fig. 1. We observe that the characteristic drop size increases only slightly as either l_1 (Fig. 2b) or l_2 (Fig. 2c) increase; moreover the drop size also increases slightly with increasing h (Fig. 2b and c).

The post-array device can emulsify fluids of a wide range of viscosities unlike conventional microfluidic devices. To illustrate this, we employ crude emulsions with dispersed and continuous phases having very different viscosities; the viscosity of the dispersed phase ranges from 1 to 10^3 times that of water, and consequently, the ratio of the viscosity of the dispersed phase to that of the continuous phase η_d/η_c ranges from 0.1 to 50. We find that, even for the fluids with high viscosities, the post-array device produces emulsion drops with a controlled average size, and in all cases, the size distribution does not depend significantly on the fluid viscosities, as shown in Fig. 3a. By contrast, the single drop microfluidic device cannot function at all with internal phase fluids of such high viscosities; this demonstrates the versatility of the post-array device.

While the fluid viscosities do not strongly influence the drop-size distributions of the emulsions produced, the device geometry does. To explore this behavior, we fabricate devices with rectangular posts of varying aspect ratios. To parameterize the drop size distribution, we measure the coefficient of variation (CV) of the drop size, defined as the standard deviation divided by the average drop size. The CV is independent of the post aspect ratio for emulsions with $\eta_d/\eta_c \leq 1$. In stark contrast, the CV increases considerably with increasing post aspect ratio for emulsions with $\eta_d/\eta_c \gg 1$, as shown in Fig. 3b. To elucidate the physical origin of this behavior, we use a high-speed camera (Phantom V9 Foam) operating at 1000 frames per second to monitor the process of drop break up. For emulsions with $\eta_d/\eta_c \leq 1$, we do not observe a significant difference in the mechanism by which drops break up in devices having either square posts, or rectangular posts oriented transverse to the imposed flow direction. This behavior is exemplified by the micrographs shown in Fig. 4a–b and Movies S1–S2,[†] and is consistent with the lack of change in the measured drop-size distributions. By contrast, while the

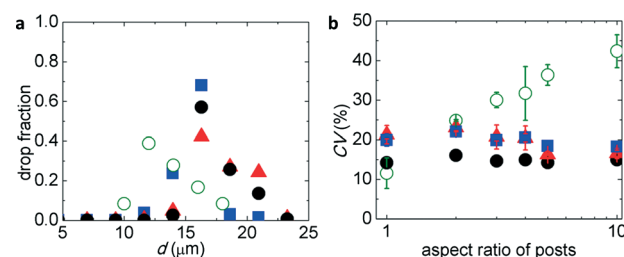


Fig. 3 Influence of the fluid viscosities on the drop size distribution. (a) The size of drops exiting the post-array device is shown for emulsions with $\eta_d/\eta_c = 50$ (○), 6.3 (●), 1.0 (▲), and 0.1 (■). The device has square posts, is $40 \mu\text{m}$ tall, has $l_1 = 40 \mu\text{m}$ and $l_2 = 20 \mu\text{m}$. (b) Influence of the aspect ratio of posts on the polydispersity of drops is shown. The error bars indicate the variance of CVs of emulsions formed in different devices of the same type. All devices are operated at $Ca > 0.03$.

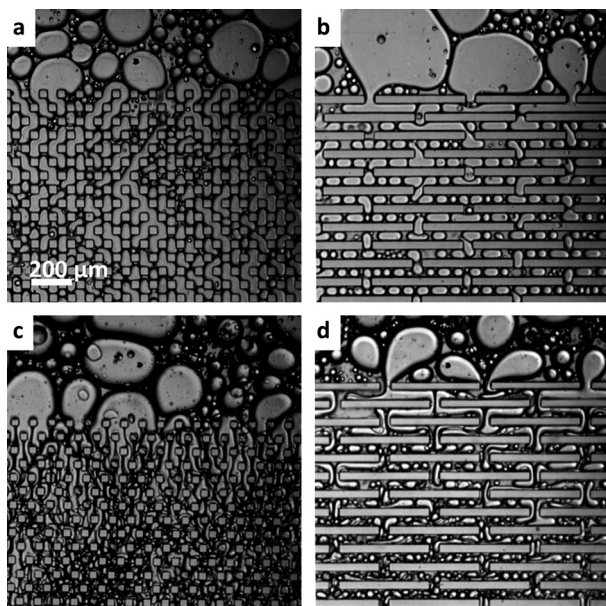


Fig. 4 Optical micrographs of post-array devices. Emulsions with (a, b) $\eta_d/\eta_c = 1$ and (c, d) $\eta_d/\eta_c = 50$ are processed in devices with (a, c) square posts or (b, d) rectangular posts with an aspect ratio of 10. Devices are operated at 5 ml h^{-1} and therefore at $Ca > 0.03$. Flow direction is from top to bottom.

drops of an emulsion with $\eta_d/\eta_c \gg 1$ readily break up in devices having square posts, they do not break up in devices with rectangular posts; instead, they form long threads that flow along the walls of the posts. This behavior is exemplified by the micrographs shown in Fig. 4c–d and Movies S3–S4† and accounts for the large increase in polydispersity.

To further explore the role of the post geometry, we investigate the behavior as the shape of the posts is varied: we fabricate posts with circular, triangular, square, and rectangular shapes, as well as combinations thereof. Interestingly, the CV strongly depends on the post shape; it is lowest for square posts (CV = 13%), and largest for posts that are concave (CV = 22%), as shown in Table 1. Upon impacting a rectangular post, drops are forced to change the flow direction by 90° ; this change in the flow direction can be either clockwise or counter clockwise. By analogy to the microfluidic drop splitting device,¹² drops typically flow in both directions simultaneously, and the resultant extensional flow causes them to split into two daughter drops. By contrast, drops that are pushed against concave posts are trapped in the cavity until they are pushed out by a subsequent drop; as a result, their shape is not strongly deformed since they are, typically, pushed towards one side of the post rather than being forced to simultaneously flow in both directions. As a result, there is significantly less extensional flow and hence less efficient drop breakage; this is reflected in the higher polydispersity of drops produced in devices with concave posts.

The drops of the crude input emulsion must be broken up many times until their size falls below a characteristic value that no longer changes. This requires a minimum number of

Table 1 Influence of the post shape on the drop size distribution

		l_1 (μm)	l_2 (μm)	Drop diameter (μm)	CV (%)
Square		40	20	28	13
Bar with aspect ratio 10		40	40	35	15
Inverse triangle		20	20	19	15
Diamond		40	0	16	15
Concave post		40	0	19	15
Circle		40	20	21	15
Diamond		40	20	21	16
Inverse triangle		40	20	19	17
Concave post		40	40	21	19
Diamond		40	40	23	19
Triangle		20	20	26	21
Triangle		40	20	28	20
Concave post		40	20	23	22

rows of posts. To determine this threshold, we fabricate devices with different numbers of rows; each row has square posts that are $40 \mu\text{m}$ tall, the inter-post distance $l_1 = 40 \mu\text{m}$, and the inter-row distance $l_2 = 20 \mu\text{m}$. Both the average drop size and the coefficient of variation decrease with increasing row number but eventually reach constant values after approximately 50 rows, as shown in Fig. 5a–b.

For emulsions produced from a device with more than 50 rows of posts, the final drop size distribution is determined by the geometry of the device. Therefore, we expect it to be independent of the drop size distribution of the input crude emulsion. To test this expectation, we use three different batches of input emulsions: a polydisperse emulsion

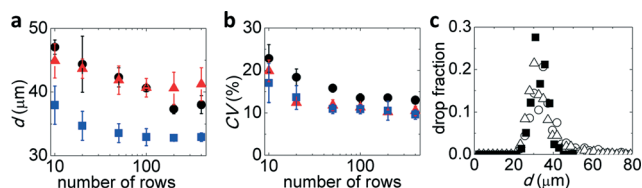


Fig. 5 (a, b) Influence of the number of rows of posts on the (a) average size and (b) polydispersity of drops of emulsions with $\eta_d/\eta_c = 6.3$ (●), 1.0 (▲), and 0.1 (■). (c) Size distribution of drops of emulsions with $\eta_d/\eta_c = 6.3$ after exiting 40 μm tall post-array devices with $l_1 = 40$ μm , and $l_2 = 20$ μm . Initial emulsions are prepared by mechanical agitation; this results in polydisperse drops (■). In addition, we produce monodisperse drops with a diameter of 70 μm (○) and 100 μm (△) using microfluidic techniques. All devices are operated at $Ca > 0.03$. The error bars indicate the variance in the drop size and size distribution of emulsions processed in different devices with identical geometries.

prepared by mechanical agitation, and two monodisperse emulsions, with drops of diameter 70 μm or 100 μm , produced using microfluidic drop makers. Consistent with our expectation, the polydispersity of the drops produced from the post-array device is independent of the size distribution of the input drops, as shown in Fig. 5c.

To enhance the throughput, we increase the number of columns of posts and have used devices with as many as 300 columns of posts. To ensure that the crude input emulsion is uniformly distributed among the different columns as it is injected into the device, we use a larger inlet channel that is 140 μm tall and 1.9 mm wide. This high throughput device is shown schematically in Fig. 6a. To demonstrate the utility of this device, we use it to produce polymeric microparticles. As the input, we use an oil-in-water (O/W) emulsion having a methacrylate-based siloxane monomer as the oil phase; this has a viscosity of 800 mPa s. We also include a photoinitiator to initiate polymerization of the oil and quickly solidify the dispersed oil phase after the emulsion exits the device by exposing it to UV light, thereby forming microparticles. The continuous aqueous phase contains 10 wt% poly(vinyl alcohol) (PVA) as a surfactant, and has a viscosity of 16 mPa s.

We push this crude emulsion through the post-array device at a flow rate of 50 ml h^{-1} ; this forms small drops of

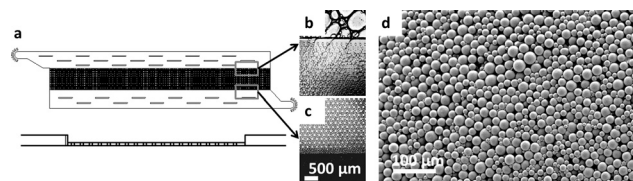


Fig. 6 Scale-up of the post-array device. (a) Schematic of the top view (top) and cross section (bottom) of a post-array device that contains 300 columns and 40 rows of square posts. Optical micrographs of the (b) inlet and (c) outlet of this device in operation are shown. Flow is from top to bottom. (d) A SEM micrograph of PDMS based microparticles produced using this device at a throughput of 15 g h^{-1} .

the oil, as shown in Fig. 6b–c and Movies S5 and S6.† We illuminate these drops with UV light as they exit the device, and wash the resultant microparticles with deionized water. The microparticles have an average diameter of 20 μm and a CV of 20%, as measured using scanning electron microscopy (SEM); a representative micrograph is shown in Fig. 6d. The post-array device produces drops at a rate of $\sim 250 \text{ l h}^{-1} \text{ m}^{-2}$; this throughput is similar to that obtained with membrane filters of $350 \text{ l h}^{-1} \text{ m}^{-2}$. However, the CV of the size of drops produced in the post-array device can be as low as 13% whereas that of drops produced with membrane filters is around 23%.⁶

Conclusions

The microfluidic post-array device enables the high throughput production of single emulsion drops of a controlled average size from fluids having a broad range of viscosities. Unlike other microfluidic methods, it can be used to emulsify fluids as much as 10^3 more viscous than water. We use this method to form drops of a viscous monomer solution, which we then solidify, thus generating polymeric microparticles. This device itself has dimensions of 24 mm \times 6 mm \times 5 mm; thus a volume of $10 \times 10 \times 10 \text{ cm}^3$, or one litre, can contain as many as 1500 devices, which can produce up to 45 litres of drop phase per hour. Therefore, it is possible to produce more than 2000 tons of drops per year using a volume of only a litre and only a single pump. Thus the post-array microfluidic device has the potential for being practical for the production of drops and microparticles at industrial scales.

Acknowledgements

This work was financially supported by the Harvard MRSEC (DMR-0820484), the NSF (DMR-1310266), and Capsum. The microfluidic devices were fabricated in the soft materials clean room of the Center for Nanoscale Systems (CNS), a member of the National Nanotechnology Infrastructure Network (NNIN), which is supported by the National Science Foundation under NSF award no. ECS-0335765. CNS is part of Harvard University. We thank Evonik Industries AG for the methacrylate based monomer solutions. SSD was funded through support from ConocoPhillips.

References

- 1 R. Mezzenga, P. Schurtenberger, A. Burbidge and M. Michel, *Nat. Mater.*, 2005, 4, 729–740.
- 2 H. Chen, Y. Zhao, J. Li, M. Guo, J. Wan, D. A. Weitz and H. A. Stone, *Lab Chip*, 2012, 11, 2312–2315.
- 3 A. R. Abate, M. Kutsovsky, S. Seiffert, M. Windbergs, L. F. V. Pinto, A. Rotem, A. S. Utada and D. A. Weitz, *Adv. Mater.*, 2011, 23, 1757–1760.

- 4 A. S. Utada, L. Y. Chu, A. Fernandez-Nieves, D. R. Link, C. Holtze and D. A. Weitz, *MRS Bull.*, 2007, **32**, 702–708.
- 5 C. Holtze, *J. Phys. D: Appl. Phys.*, 2013, **46**, 114008.
- 6 M. M. Dragosavac, G. T. Vladisavljevic, R. G. Holdich and M. T. Stillwell, *Langmuir*, 2011, **28**, 134–143.
- 7 G. T. Vladisavljevic, I. Kobayashi and M. Nakajima, *Microfluid. Nanofluid.*, 2012, **13**, 151–178.
- 8 M. K. Mulligan and J. P. Rothstein, *Microfluid. Nanofluid.*, 2012, **13**, 65–73.
- 9 S. Protiere, M. Z. Bazant, D. A. Weitz and H. A. Stone, *Europhys. Lett.*, 2010, **92**, 54002.
- 10 P. Garstecki, M. J. Fuerstman, H. A. Stone and G. M. Whitesides, *Lab Chip*, 2006, **6**, 437–446.
- 11 A. R. Abate, A. Poitzsch, Y. Hwang, J. Lee, J. Czerwinska and D. A. Weitz, *Phys. Rev. E: Stat., Nonlinear, Soft Matter Phys.*, 2009, **80**, 026310.
- 12 D. R. Link, S. L. Anna, D. A. Weitz and H. A. Stone, *Phys. Rev. Lett.*, 2004, **92**, 054503.